Models for the two-phase flow of concentrated suspensions

TOBIAS AHNERT[1], ANDREAS MÜNCH[2] and BARBARA WAGNER[1]

[1] *Institute of Mathematics, Technische Universität Berlin, Strasse des 17. Juni 136, 10623 Berlin, Germany*
email: `ahnert@math.tu-berlin.de`
[2] *Mathematical Institute, 24–29 St Giles, Oxford OX1 3LB, UK*

A new two-phase model for concentrated suspensions is derived that incorporates a constitutive law combining the rheology for non-Brownian suspension and granular flow. The resulting model naturally exhibits a Bingham-type flow property. This property is investigated in detail for the simple geometry of plane Poiseuille flow, where an unyielded or jammed zone of finite width arises in the center of the channel. For the steady state of this problem, the governing equation are reduced to a boundary value problem for a system of ordinary differential equations and the dependence of its solutions are analyzed by using phase-space methods. For the general time-dependent case a new drift-flux model is derived for the first time using matched asymptotic expansions that take account of the boundary layers at the walls and the interface between the yielded and unyielded region. Using the drift-flux model, the behavior of the suspension flow, in particular the appearance and evolution of unyielded or jammed regions is then studied numerically for different choices of the parameters.

Key Words: Suspensions, jamming, yield stress, averaging, multiphase model, phase-space methods, matched asymptotics, drift-flux

1 Introduction

Ever since the derivation of an effective viscosity for dilute suspensions by Einstein [12] and its extensions by Batchelor & Green [1], there has been numerous investigations into their rheological properties. In particular since the experimental work by Gadala-Maria & Acrivos [13] new physical phenomena such as shear-induced particle migration for concentrated suspensions, spurred many theoretical investigations that led to expressions for associated diffusive flux terms as well as drift-flux models, see for example [20, 26, 6, 23].

While drift-flux models are quite popular and are frequently combined as a transport mechanism [7, 24, 33], they do predict also unphysical migration behavior. For example in the case of channel flow these models predict a sharp peak in the particle volume fraction profile in the center of the channel, where the shear rate vanishes [25], whereas

in experiments such as for example by Hampton [14] the concentration profile is in fact flattened there. While these issues were addressed by introducing concepts of "viscous temperature" [25, 18], or by slightly changing parameter values such as the exponent in the Krieger-Dougherty law or in the expressions for the relative suspension viscosity and the particulate phase pressure as the maximum packing fraction is approached [28], it remains to understand how these models can be based on their underlying two-phase models.

In addition, as has been shown in Cassar et al. [5] for highly dense suspensions of particles in a viscous liquid that is sheared at a rate $\dot{\gamma}$ under a confining pressure p_p can be characterized by a single dimensionless control parameter, the "viscous number" $I_v = \eta_f \dot{\gamma}/p_p$, where η_f is the fluid viscosity. These findings have been supported by experiments where the suspensions are sheared with a constant particle pressure [2]. Their results show that, indeed, the friction and volume-fraction law collapse onto universal curves when expressed in terms of the dimensionless number I_v. By including hydrodynamic contributions, Boyer et al. propose a model for the whole range of I_v, which has been discussed by [8], and also by Trulsson et al. [30]. An earlier review of stress terms for dense suspensions can be found in [29].

Boyer et al. formulate their model in a form for suspensions, where the shear stress and particle pressure are expressed in terms of the strain rate and the volume fraction. Their expressions for the shear and normal viscosities are similar to the ones found in Morris & Boulay [23], and also Miller et al. [22], who investigated more general curvilinear flows, where the migration behavior was accommodated by allowing for anisotropy in the normal stresses. Hence, both models should exhibit viscoplastic behavior with a yield stress that is proportional to the particle pressure.

The focus of the present study is to incorporate the rheology of Boyer et al. into a derivation of new drift-flux model for dense suspensions. Our derivation starts with derivation of a new two-phase model for non-homogeneous shear flows that captures the flow properties of non-Brownian dense suspensions by including the constitutive equations proposed by Boyer et al. [2]. The derivation of our two-phase model is based on the averaging framework as given in Drew & Passman [9, 10].

In order to investigate the flow behavior predicted by this two-phase model as the particle volume fraction is varied, we choose the pressure-driven plane Poiseuille flow as our basic model example for non-constant shear flows.

We first investigate the stationary solutions for which the problem reduces to a boundary-value problem for a system of ordinary differential equations. Using phase-space methods we show existence of solutions that show an unyielded or jammed region with maximum volume fraction in the center of the channel and naturally exhibits Bingham-type flow properties. We then study the dependence of the width of the jammed region and the corresponding flow field upon varying the flow parameters.

For typical ranges of the parameter $Da = L/K_p = O(1/\varepsilon)$, where L is the characteristic scale of the channel width and K is proportional to the particle size, a matched asymptotic analysis shows moreover that the flow field develops a boundary layer at the channel walls and the interface between the unyielded and yielded region.

We generalize this analysis and for the first time present a systematic derivation of a drift-flux model via matched asymptotics. Using this model we show numerically the

emergence of the unyielded region in the flow and its evolution towards the stationary state.

2 Formulation of a two-phase model

We consider two inert phases and denote with $k \in \{s, f\}$ the solid phase by s and the liquid phase by f. Inside each phase the balance equations for mass and momentum

$$\partial_t \rho + \nabla \cdot (\rho \boldsymbol{u}) = 0 \tag{2.1}$$

$$\partial_t(\rho \boldsymbol{u}) + \nabla \cdot (\rho \boldsymbol{u} \otimes \boldsymbol{u}) - \nabla \cdot \boldsymbol{T} - \boldsymbol{f} = \boldsymbol{0} \tag{2.2}$$

are satisfied together with the two jump conditions (see e.g. [17])

$$\sum_k \rho_k (\boldsymbol{u}_k - \boldsymbol{u}_i) \cdot \boldsymbol{n}_k = 0 \tag{2.3}$$

$$\sum_k \rho_k \boldsymbol{u}_k (\boldsymbol{u}_k - \boldsymbol{u}_i) \cdot \boldsymbol{n}_k - \boldsymbol{T}_k \cdot \boldsymbol{n}_k = \sigma_{fs} \kappa \boldsymbol{n}_s, \tag{2.4}$$

at the interfaces of the phases with $\boldsymbol{n}_k$ denoting the unit normal pointing out of phase k, σ_{fs} a surface tension coefficient and κ the curvature of the interface that is positive towards $-\boldsymbol{n}_s$; $\boldsymbol{u}_i$ is the interface velocity. The quantities ρ, $\boldsymbol{u}$, $\mathbf{T}$ and $\mathbf{f}$ denote density, velocity, stress tensor and body force density in each phase, respectively. At an interface $\boldsymbol{u}_k$ is defined as

$$\boldsymbol{u}_k(\boldsymbol{x}^*, t) \equiv \lim_{\boldsymbol{x} \to \boldsymbol{x}^*; \boldsymbol{x} \in K} \boldsymbol{u}(x, t),$$

where K denotes the set of points occupied by phase k, and similarly for the other quantities.

Essentially three different averaging approaches have been pursued in the literature. The volume average, the time average and the ensemble average (sometimes also called statistical average). Although all three produce similar balance equation for the phases their derivation and closure is distinct. Besides the ensemble averaging developed by Drew & Passman in [10] and [9], volume averaging is treated in Kolev [19] and Whitaker [32] and time averaging in Ishii et al. [17].

For the derivation of our two-phase model, given in the appendix B, we follow the mathematical framework by Drew [9] and Drew and Passman [10] and obtain for the averaged quantities

$$\phi_k \equiv \langle X_k \rangle, \quad \overline{\rho}_k \equiv \frac{\langle X_k \rho \rangle}{\phi_k}, \quad \widehat{\boldsymbol{u}}_k \equiv \frac{\langle X_k \rho \boldsymbol{u} \rangle}{\phi_k \overline{\rho}_k}, \quad \overline{p}_k \equiv \frac{\langle X_k p \rangle}{\phi_k}, \quad \overline{\boldsymbol{\tau}}_k \equiv -\frac{\langle X_k \boldsymbol{\tau} \rangle}{\phi_k} \tag{2.5}$$

the following balance equations

$$\partial_t \phi_s + \nabla \cdot (\phi_s \widehat{\boldsymbol{u}}_s) = 0, \tag{2.6 a}$$

$$\partial_t \phi_f + \nabla \cdot (\phi_f \widehat{\boldsymbol{u}}_f) = 0, \tag{2.6 b}$$

$$\overline{\rho}_s \partial_t (\phi_s \widehat{\boldsymbol{u}}_s) + \nabla \cdot (\phi_s \overline{\rho}_s \widehat{\boldsymbol{u}}_s \otimes \widehat{\boldsymbol{u}}_s) \tag{2.6 c}$$

$$-\nabla \cdot (\phi_s \overline{\boldsymbol{\tau}}_s) + \nabla(\phi_s \overline{p}_s) = M_s^d + \overline{p}_f \nabla \phi_s, \tag{2.6 d}$$

$$\overline{\rho}_f \partial_t (\phi_f \widehat{\boldsymbol{u}}_f) + \nabla \cdot (\phi_f \overline{\rho}_f \widehat{\boldsymbol{u}}_f \otimes \widehat{\boldsymbol{u}}_f) \tag{2.6 e}$$

$$-\nabla \cdot (\phi_f \overline{\boldsymbol{\tau}}_f) + \nabla(\phi_f \overline{p}_f) = -M_s^d + \overline{p}_f \nabla \phi_f. \tag{2.6 f}$$

Although this model has a viscous term, it contains a well-known ill-posedness in the long-wave limit, c.f. [21, 27]. In appendix D we propose a common regularization, that does not change the asymptotic results.

2.1 Constitutive equations for a dense suspension

To close the model for the flow in the bulk, we need to specify constitutive equations besides the assumptions already made. Essentially we need four relations for the pressure difference and stress between the phases $\overline{p}_s - \overline{p}_f$ and M_s^d, and for the stresses in each phase, $\overline{\boldsymbol{\tau}}_f$ and $\overline{\boldsymbol{\tau}}_s$.

For the momentum transfer M_s^d, we use the Kozeny-Carman equation for the permeability (cf. [15] and [3]),

$$M_s^d = \frac{\mu_f \phi_s^2}{K_p \phi_f}(\widehat{\boldsymbol{u}}_f - \widehat{\boldsymbol{u}}_s), \tag{2.7}$$

where K_p is the permeability coefficient.

The constitutive law for the remaining quantities extend the model for dense suspensions given by Boyer et al. [2] for shear flow to a general flow situation. We state it in terms of the (weighted) solid contact pressure, defined here as

$$p_c \equiv \phi_s(\overline{p}_s - \overline{p}_f), \tag{2.8}$$

and the shear rate tensors for each phase

$$\dot{\boldsymbol{\gamma}}_f \equiv [\nabla \widehat{\boldsymbol{u}}_f + (\nabla \widehat{\boldsymbol{u}}_f)^T], \qquad \dot{\boldsymbol{\gamma}}_s \equiv [\nabla \widehat{\boldsymbol{u}}_s + (\nabla \widehat{\boldsymbol{u}}_s)^T]. \tag{2.9}$$

For the liquid phase stress, we have

$$\overline{\boldsymbol{\tau}}_f = \mu_f \dot{\boldsymbol{\gamma}}_f + (\mu^* - \frac{2}{3}\mu_f)(\nabla \cdot \widehat{\boldsymbol{u}}_f)\boldsymbol{I}, \tag{2.10\,a}$$

where μ_f denotes the viscosity of the pure liquid. The second term in the relation for $\overline{\boldsymbol{\tau}}_f$ will be dropped by setting the bulk viscosity $\mu^* = \frac{2}{3}\mu_f$.

For the solid phase, we need to consider two cases for the constitutive law:
Either $|\dot{\boldsymbol{\gamma}}_s| > 0$, then

$$\overline{\boldsymbol{\tau}}_s = \mu_f \eta_s(\phi_s)\dot{\boldsymbol{\gamma}}_s, \tag{2.10\,b}$$

$$p_c = \mu_f \eta_n(\phi_s)|\dot{\boldsymbol{\gamma}}_s|, \tag{2.10\,c}$$

with

$$\eta_s(\phi_s) = 1 + \frac{5}{2}\frac{\phi_{sc}}{\phi_{sc} - \phi_s} + \mu_c(\phi_s)\frac{\phi_s}{(\phi_{sc} - \phi_s)^2}, \tag{2.10\,d}$$

$$\mu_c(\phi_s) = \mu_1 + \frac{\mu_2 - \mu_1}{1 + I_0 \phi_s^2 (\phi_{sc} - \phi_s)^{-2}}, \tag{2.10\,e}$$

$$\eta_n(\phi_s) = \left(\frac{\phi_s}{\phi_{sc} - \phi_s}\right)^2, \tag{2.10\,f}$$

where for tensors $\boldsymbol{a}$ we define the norm as $|\boldsymbol{a}| = (\frac{1}{2}\sum_{j,k}|a_{jk}|^2)^{1/2}$. The material parameters $\mu_2 \geq \mu_1 > 0$, $I_0 \geq 0$ characterize the contact contribution in the expression for η_s, and ϕ_{sc} is the maximum volume fraction for the solid phase at the jamming point [2].

For $\dot{\boldsymbol{\gamma}}_s = 0$ we require

$$\phi_s = \phi_{sc}, \tag{2.10 g}$$

while $\overline{\boldsymbol{\tau}}_s$, $\overline{p}_s$ and $\overline{p}_f$ are left unspecified, except for the constraint

$$|\overline{\boldsymbol{\tau}}_s| \leq \mu_1 p_c. \tag{2.10 h}$$

Across a yield surface, by which we mean the boundary of the regions where $\dot{\boldsymbol{\gamma}}_s$ is zero, and for which $\boldsymbol{n}_y$ denotes the unit normal vector, we require ϕ_s, ϕ_f, $\widehat{\boldsymbol{u}}_f$, $\widehat{\boldsymbol{u}}_s$, $(-\overline{p}_f \boldsymbol{I} + \overline{\boldsymbol{\tau}}_f) \cdot \boldsymbol{n}_y$, $(-\overline{p}_s \boldsymbol{I} + \overline{\boldsymbol{\tau}}_s) \cdot \boldsymbol{n}_y$ and $|\dot{\boldsymbol{\gamma}}_s|$ to be continuous.

2.2 Non-dimensionalization

We introduce characteristic scales via

$$x = Lx', \qquad y = Ly', \qquad z = Lz', \tag{2.11}$$

$$t = \frac{L}{U}t', \qquad \boldsymbol{u}_k = U\boldsymbol{u}'_k, \qquad p_k = \frac{U\mu_f}{L}p'_k, \tag{2.12}$$

for $k = s$, f. After non-dimensionalization, we drop the primes and also the bars and hats indicating averaging, and obtain the system

$$\partial_t \phi_f + \nabla \cdot (\phi_f \boldsymbol{u}_f) = 0, \tag{2.13 a}$$

$$\partial_t \phi_s + \nabla \cdot (\phi_s \boldsymbol{u}_s) = 0, \tag{2.13 b}$$

$$\text{Re}[\partial_t(\phi_f \boldsymbol{u}_f) + \nabla \cdot (\phi_f \boldsymbol{u}_f \otimes \boldsymbol{u}_f)] \tag{2.13 c}$$

$$-\nabla \cdot (\phi_f \boldsymbol{\tau}_f) + \phi_f \nabla p_f = -\text{Da}\frac{\phi_s^2}{\phi_f}(\boldsymbol{u}_f - \boldsymbol{u}_s),$$

$$\frac{\text{Re}}{r}[\partial_t(\phi_s \boldsymbol{u}_s) + \nabla \cdot (\phi_s \boldsymbol{u}_s \otimes \boldsymbol{u}_s)] \tag{2.13 d}$$

$$-\nabla \cdot (\phi_s \boldsymbol{\tau}_s) + \phi_s \nabla p_f + \nabla p_c = \text{Da}\frac{\phi_s^2}{\phi_f}(\boldsymbol{u}_f - \boldsymbol{u}_s).$$

Three dimensionless numbers appear here, namely the Reynolds number $\text{Re} = \frac{UL\rho_f}{\mu_f}$,, the Darcy number $\text{Da} = \frac{L^2}{K_p}$ and the density ratio $r = \frac{\rho_f}{\rho_s}$. We focus on the case, where liquid and solid phases are density matched i.e. $r = 1$.

The non-dimensional versions of the constitutive equations for the rheology are now as follows: For the liquid phase, we have

$$\boldsymbol{\tau}_f = \dot{\boldsymbol{\gamma}}_f. \tag{2.14 a}$$

For the solid phase, either $|\dot{\boldsymbol{\gamma}}_s| > 0$, then

$$\boldsymbol{\tau}_s = \eta_s(\phi_s)\dot{\boldsymbol{\gamma}}_s, \tag{2.14 b}$$

$$p_c = \eta_n(\phi_s)|\dot{\boldsymbol{\gamma}}_s|, \tag{2.14 c}$$

with (2.10 d)-(2.10 f); or $\dot{\boldsymbol{\gamma}}_s = 0$, and then we require
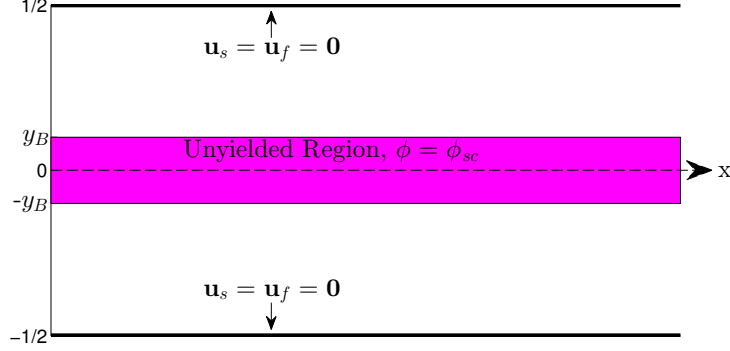
$$\phi_s = \phi_{sc}$$

FIGURE 1. Sketch of the flow situation in a channel.

and

$$|\boldsymbol{\tau}_s| \leq \mu_1 p_c.$$

The continuity conditions across yield surfaces carry over from the dimensional equations and also the parameters, μ_1, μ_2 and I_0 and ϕ_{sc}, which were non-dimensional to begin with.

Remark

Let us note that in the near-critical, or jamming limit, when $\phi_s \to \phi_{sc}$, and for fixed contact pressure $p_c = \phi_s(p_s - p_f)$, it follows from $(2.14\,c)$, $(2.10\,f)$ that $\dot{\boldsymbol{\gamma}}_s$ tends to zero as $O((\phi_{sc} - \phi_s)^2)$. Thus, the solid phase velocity $\boldsymbol{u}_s$ becomes uniform, so that in a conveniently chosen reference frame, it is at rest. Notice, however, that $|\boldsymbol{\tau}_s| \to \mu_1 p_c$ remains $O(1)$ due to $(2.14\,b)$, $(2.10\,d)$, $(2.10\,e)$. The equations for the liquid phase become

$$\nabla \cdot \boldsymbol{u}_f = 0,$$

$$\mathrm{Re}\left[\partial_t \boldsymbol{u}_f + \nabla \cdot (\boldsymbol{u}_f \otimes \boldsymbol{u}_f)\right] = -\nabla p_f + \nabla \cdot \dot{\boldsymbol{\gamma}}_f - \mathrm{Da}\,\frac{\phi_s^2}{\phi_f^2}(\boldsymbol{u}_f - \boldsymbol{u}_s).$$

If, in addition, $\mathrm{Da} \to \infty$, the term $\nabla \cdot \dot{\boldsymbol{\gamma}}_f$ and the inertia terms drop out from the second equation and we recover Darcy's law in a porous medium.

3 Plane Poiseuille flow

It is instructive to investigate the properties of the model (2.13) for one of the classical flow situations, namely, plane Poiseuille or channel flow.

We suppose the dimensions of the channel are $0 < x < L$ and $-\frac{1}{2} < y < \frac{1}{2}$ and prescribe for the inlet conditions at $x = 0$

$$\phi_s = \phi_{s,in}, \quad \boldsymbol{u}_f = \begin{pmatrix} u_{f,in}\left(\frac{1}{4} - y^2\right) \\ 0 \end{pmatrix}, \quad \boldsymbol{u}_s = \begin{pmatrix} u_{s,in}\left(\frac{1}{4} - y^2\right) \\ 0 \end{pmatrix} \tag{3.1}$$

and for the outlet condition at $x = L$

$$\mathbf{n} \cdot (p_s \boldsymbol{I} + \phi_s \eta_s (\nabla \boldsymbol{u}_s)^T) = 0, \quad \mathbf{n} \cdot (p_f \boldsymbol{I} + \phi_f \eta_s (\nabla \boldsymbol{u}_s)^T) = 0. \tag{3.2}$$

In addition we assume that inertial effects are negligible and hence obtain for the bulk equations

$$\partial_t \phi_f + \nabla \cdot (\phi_f \boldsymbol{u}_f) = 0, \tag{3.3 a}$$

$$\partial_t \phi_s + \nabla \cdot (\phi_s \boldsymbol{u}_s) = 0, \tag{3.3 b}$$

$$-\nabla \cdot (\phi_f \boldsymbol{\tau}_f) + \phi_f \nabla p_f = -\mathrm{Da} \frac{\phi_s^2}{\phi_f} (\boldsymbol{u}_f - \boldsymbol{u}_s), \tag{3.3 c}$$

$$-\nabla \cdot (\phi_s \boldsymbol{\tau}_s) + \phi_s \nabla p_f + \nabla p_c = \mathrm{Da} \frac{\phi_s^2}{\phi_f} (\boldsymbol{u}_f - \boldsymbol{u}_s), \tag{3.3 d}$$

$$\phi_f + \phi_s = 1, \tag{3.3 e}$$

where

$$\boldsymbol{\tau}_f = \dot{\boldsymbol{\gamma}}_f \tag{3.4 a}$$

$$|\boldsymbol{\tau}_s| \leq \mu_1 p_c, \qquad \phi_s = \phi_{sc} \qquad \text{if } |\dot{\boldsymbol{\gamma}}_s| = 0 \tag{3.4 b}$$

$$\boldsymbol{\tau}_s = \eta_s(\phi_s)\dot{\boldsymbol{\gamma}}_s, \qquad p_c = \eta_n(\phi_s)|\dot{\boldsymbol{\gamma}}_s| \qquad \text{if } |\dot{\boldsymbol{\gamma}}_s| \neq 0. \tag{3.4 c}$$

At the channel walls we assume the no-slip conditions

$$\boldsymbol{u}_s = \boldsymbol{0}, \qquad \boldsymbol{u}_f = \boldsymbol{0}. \tag{3.5}$$

For the two-phase model at hand, it turns out to be advantageous to formulate the problem in terms of the flow variables

$$\boldsymbol{v} \equiv \phi_f \boldsymbol{u}_f + \phi_s \boldsymbol{u}_s, \qquad \boldsymbol{w} \equiv \boldsymbol{u}_f - \boldsymbol{u}_s. \tag{3.6}$$

In these variables, noting that $\boldsymbol{v} + \phi_s \boldsymbol{w} = \boldsymbol{u}_f$, $\boldsymbol{v} - \phi_f \boldsymbol{w} = \boldsymbol{u}_s$ and using $\phi_f = 1 - \phi_s$ the problem can be written as

$$\nabla \cdot \boldsymbol{v} = 0 \tag{3.7 a}$$

$$\partial_t \phi_s + \nabla \cdot (\phi_s \boldsymbol{v} - \phi_s(1 - \phi_s)\boldsymbol{w}) = 0 \tag{3.7 b}$$

$$-\nabla \cdot \left((1 - \phi_s)\dot{\boldsymbol{\gamma}}_f\right) + (1 - \phi_s)\nabla p_f = -\mathrm{Da} \frac{\phi_s^2}{1 - \phi_s} \boldsymbol{w} \tag{3.7 c}$$

$$-\nabla \cdot (\phi_s \eta_s \dot{\boldsymbol{\gamma}}_s) + \phi_s \nabla p_f + \nabla(\eta_n |\dot{\boldsymbol{\gamma}}_s|) = \mathrm{Da} \frac{\phi_s^2}{1 - \phi_s} \boldsymbol{w} \tag{3.7 d}$$

and with no-slip conditions at the walls $y = \pm\frac{1}{2}$

$$\boldsymbol{v} = \boldsymbol{0}, \qquad \boldsymbol{w} = \boldsymbol{0}. \tag{3.7 e}$$

3.1 Phase space analysis of the stationary problem

For the system $(3.7\,a)$-$(3.7\,e)$ we derive conditions for the existence of stationary two-dimensional solutions where all quantities, except for the pressure, depend only on y. In addition, from now on we set $\phi_s \equiv \phi$

$$\phi = \phi(y), \qquad \boldsymbol{v} = \boldsymbol{v}(y), \qquad \boldsymbol{w} = \boldsymbol{w}(y), \tag{3.8}$$

$$\boldsymbol{\tau}_f = \boldsymbol{\tau}_f(y), \qquad \boldsymbol{\tau}_s = \boldsymbol{\tau}_s(y), \qquad p_f = p_f(x, y). \tag{3.9}$$

The combination of no-slip boundary conditions $(3.7\,e)$ with $(3.7\,a)$, $(3.7\,b)$ yields (if v_1, v_2 and w_1, w_2 denote the components of the vectors $\boldsymbol{v}$ and $\boldsymbol{w}$, respectively)

$$v_2 = 0, \qquad\qquad\qquad w_2 = 0, \qquad\qquad (3.10)$$

and therefore

$$\dot{\boldsymbol{\gamma}}_s = \begin{pmatrix} 0 & \partial_y(v_1 - (1-\phi)w_1) \\ \partial_y(v_1 - (1-\phi)w_1) & 0 \end{pmatrix}, \qquad (3.11)$$

$$\dot{\boldsymbol{\gamma}}_f = \begin{pmatrix} 0 & \partial_y(v_1 + \phi w_1) \\ \partial_y(v_1 + \phi w_1) & 0 \end{pmatrix}. \qquad (3.12)$$

The second component from $(3.7\,c)$ requires p_f to be independent of y. For the total stress $\boldsymbol{\tau} \equiv \phi_f \boldsymbol{\tau}_f + \phi_s \boldsymbol{\tau}_s$ we get from $(3.7\,c)$, $(3.7\,d)$

$$\partial_x p_f - \partial_y \tau_{12} = 0, \qquad \partial_y p_c = \partial_y(\eta_n|\dot{\boldsymbol{\gamma}}_s|) = 0. \qquad (3.13)$$

This means that in the first of these equations, one term only depends on x and the other only on y, so both have to be constant, therefore the solution is

$$p_f(x) = p_1 x + p_0, \qquad\qquad (3.14\,a)$$

where p_0 is a constant of integration, which by a choice of origin, we can assume, without loss of generality, to be zero, and

$$\tau_{12}(y) = p_1 y. \qquad\qquad (3.14\,b)$$

From now on, we will only look at the case of solutions with velocities and volume fractions that are symmetric with respect to $y = 0$ and that have at most one unyielded region for $-y_B \leq y \leq y_B$, i.e. with at most one y_B, where $0 \leq y_B \leq 1/2$. Due to the symmetry assumption, the constant contribution to τ_{12} has been set to zero in $(3.14\,b)$ and it is sufficient to consider only non-negative y. The same reasoning as above further shows

$$p_c = \text{const.} \qquad \text{if } |\dot{\boldsymbol{\gamma}}_s| > 0. \qquad (3.15)$$

Thus, the contact pressure, p_c, is a constant here, which is free and thus acts as an additional parameter.

Overall we get the system: For $y \in [y_B; 1/2]$, ϕ, τ_{s12}, τ_{f12}, v_1 and w_1 satisfy

$$\partial_y((1-\phi)\tau_{f\,12}) = (1-\phi)p_1 + \text{Da}\,\frac{\phi^2}{1-\phi}w_1, \qquad (3.16\,a)$$

$$\phi_s \tau_{s12} = p_1 y - (1-\phi)\tau_{f12}, \qquad\qquad (3.16\,b)$$

$$\partial_y w = \tau_{f12} - \frac{\tau_{s12}}{\eta_s(\phi)}, \qquad\qquad (3.16\,c)$$

$$p_c = \eta_n(\phi)|\partial_y(v_1 - (1-\phi)w_1)|. \qquad\qquad (3.16\,d)$$

In the unyielded region $y \in [0; y_B[$, equations $(3.16\,a)$-$(3.16\,b)$ stay the same, but the two remaining ones are replaced by

$$\partial_y(v_1 - (1-\phi)w_1) \equiv \partial_y u_s = 0 \qquad \text{and} \qquad \phi = \phi_{sc}. \qquad (3.16\,e)$$

The boundary conditions are the no-slip

$$v_1 = 0, \quad w_1 = 0, \qquad \text{at } y = 1/2, \qquad (3.16\,f)$$

and symmetry conditions

$$\partial_y v_1 = 0, \quad \partial_y w_1 = 0, \qquad \text{at } y = 0. \qquad (3.16\,g)$$

In case the unyielded region fills out the whole channel, i.e. $y_B = 1/2$, the no-slip boundary conditions together with $(3.16\,e)$ gives $u_s = 0$. Then $(3.16\,a)$ becomes the Brinkman equation, c.f. [4]. For the yield surface at $y = y_B$ we demand the continuity conditions

$$[\tau_{s12}]_-^+ = 0, \qquad\qquad [\tau_{f12}]_-^+ = 0, \qquad\qquad [v_1]_-^+ = 0, \qquad (3.16\,h)$$

$$[w_1]_-^+ = 0, \qquad\qquad [\phi]_-^+ = 0, \qquad\qquad (3.16\,i)$$

where we denote $[g]_-^+ = \lim_{y \searrow y_B} g - \lim_{y \nearrow y_B} g$. We remark that these conditions are not all independent, as, for example, the second condition in $(3.16\,g)$ can be obtained from the first via $(3.16\,e)$, and the continuity of one of the stresses in $(3.16\,i)$ implies the other via $(3.16\,b)$.

Notice that $(3.16\,d)$ applies in the region $[y_B; 1/2]$ where $\dot{\boldsymbol{\gamma}}_s > 0$, so that, if $p_c = 0$, this implies $\phi = 0$, i.e. no solid phase, which seems equivocal. We therefore assume $p_c > 0$. Then, we can remove p_c from the equations by rescaling

$$\tau_{s12} = p_c \tilde{\tau}_{s12}, \qquad\qquad \tau_{f12} = p_c \tilde{\tau}_{s12}, \qquad\qquad p_1 = p_c \tilde{p}_1, \qquad (3.17)$$

$$u_f = p_c \tilde{u}_f, \qquad\qquad u_s = p_c \tilde{u}_s. \qquad\qquad (3.18)$$

The fact that p_c can be scaled out of the problem in this way implies that the width of the unyielded region i.e. y_B does not depend on p_c, as was reported in [16]. We note that in conventional Herschel-Bulkley models, which are also able to capture yield stress and shear-thinning, the unyielded region would change with p_c.

3.1.1 *Phase space analysis*

Using phase-space methods, we ask if for system (3.16) solutions exist and under which conditions, but first we will reduce the system into a second order, non-autonomous system of ordinary differential equations for $w \equiv w_1$ and ϕ.

We first note that in the fluid region $y \in [y_B; 1/2]$ combining the definition of the solid stress $(3.4\,c)$ and $(3.16\,d)$ yields

$$\phi\tau_{s12} = \phi\eta_s \partial_y u_s = \frac{\phi\eta_s}{\eta_n}\text{sign}(\partial_y u_s) = -\frac{\phi\eta_s}{\eta_n}\text{sign}(y), \qquad (3.19)$$

where we have made the assumption that $\text{sign}(\partial_y u_s) = \text{sign}(\boldsymbol{\tau}) = -\text{sign}(y)$ holds. This assumption is fundamental and based on the experimental observation, that channel velocity curves are roughly square profiles (c.f. [14]) and is further asserted by $(3.14\,b)$, which states that the total stress is just a linear function. Since Da is large, we expect $\boldsymbol{u}_s \approx \boldsymbol{u}$ and this behavior should also be true for the solid velocity.

Then using $(3.16\,b)$ in $(3.16\,a)$ and (3.19) yields

$$\partial_y N(\phi) = -\phi p_1 + \text{Da}\frac{\phi^2}{1-\phi}w, \qquad (3.20\,a)$$

which will be used as an equation for the solid volume fraction. We get an equation for w by combing (3.16 b) and (3.16 c) to give

$$\partial_y w = \frac{p_1 y + N(\phi)}{1 - \phi} + \frac{1}{\eta_n(\phi)}. \tag{3.20 b}$$

The function N is given by

$$N(\phi) \equiv \frac{\phi \eta_s(\phi)}{\eta_n(\phi)}. \tag{3.20 c}$$

In the unyielded region $y \in [0; y_B[$ we already know

$$\phi = \phi_{sc} \tag{3.20 d}$$

and since $\partial_y u_s = 0$, we have $\tau_{f12} = \partial_y u_f = \partial_y w$, which together with (3.16 a) is

$$\partial_{yy} w = p_1 + \mathrm{Da} \frac{\phi_{sc}^2}{(1 - \phi_{sc})^2} w. \tag{3.20 e}$$

At the channel wall and center, we have the boundary conditions

$$w = 0 \qquad\qquad \text{at } y = 1/2, \tag{3.20 f}$$

$$\partial_y w = 0 \qquad\qquad \text{at } y = 0, \tag{3.20 g}$$

and at the yield surface,

$$\phi = \phi_{sc}, \quad [w]_-^+ = 0, \quad [w_y]_-^+ = 0, \quad \text{at } y = y_B. \tag{3.20 h}$$

The problem for w in the unyielded region, (3.20 e) and (3.20 g), can be solved explicitly. For $\mathrm{Da} > 0$, we have

$$w = \alpha_1 \cosh\left(\frac{\mathrm{Da}^{1/2} \phi_{sc}}{1 - \phi_{sc}} y\right) - \frac{(1 - \phi_{sc})^2}{\mathrm{Da}\, \phi_{sc}^2} p_1, \tag{3.21}$$

where α_1 is a constant of integration. We can use this in the last two conditions in (3.20 h) to get

$$\partial_y w = \left(w + \frac{(1 - \phi_{sc})^2}{\mathrm{Da}\, \phi_{sc}^2} p_1\right) \frac{\mathrm{Da}^{1/2} \phi_{sc}}{1 - \phi_{sc}} \tanh\left(\frac{\mathrm{Da}^{1/2} \phi_{sc}}{1 - \phi_{sc}} y_B\right), \text{ at } y = y_B \tag{3.22}$$

and from this a new formulation of the free boundary condition

$$\phi = \phi_{sc}, \tag{3.23 a}$$

$$w = W(y_B) \equiv \frac{p_1 y_B + \mu_1}{\mathrm{Da}^{1/2} \phi_{sc} \tanh\left(\frac{\mathrm{Da}^{1/2} \phi_{sc}}{1 - \phi_{sc}} y_B\right)} - \frac{(1 - \phi_{sc})^2}{\mathrm{Da}\, \phi_{sc}^2} p_1, \quad \text{at } y = y_B. \tag{3.23 b}$$

We have thus reduced the problem to a free boundary value problem for second order system of ODEs (3.20 a), (3.20 b) with a condition (3.20 f) at the fixed boundary and two at the free boundary (3.23 a), (3.23 b).

For the solution of the boundary value problem (3.20), we proceed as follows. Rewriting (3.20 a) for w, i.e.

$$w = \frac{(\partial_y N + \phi\, p_1)(1 - \phi)}{\mathrm{Da}\, \phi^2}, \tag{3.24}$$

and using it in (3.20 *b*) and the boundary conditions yields an equation solely in ϕ, i.e.

$$\partial_y \left(\frac{(\partial_y N + \phi\, p_1)\,(1 - \phi)}{\mathrm{Da}\,\phi^2} \right) = \frac{p_1 y + N}{1 - \phi} + \frac{1}{\eta_n}, \qquad (3.25\,a)$$

with boundary conditions

$$0 = \partial_y N + \phi_s\, p_1 \qquad\qquad \text{at } y = \frac{1}{2}, \qquad (3.25\,b)$$

$$\phi = \phi_{sc} \qquad\qquad \text{at } y = y_B, \qquad (3.25\,c)$$

$$\frac{(\partial_y N + p_1)\,(1 - \phi_{sc})}{\mathrm{Da}\,{\phi_{sc}}^2} = \frac{p_1 y_B + \mu_1}{\mathrm{Da}^{\frac{1}{2}} \phi_{sc} \tanh\left(\frac{\mathrm{Da}^{\frac{1}{2}} \phi_{sc}}{1 - \phi_{sc}} y_B \right)} \qquad \text{at } y = y_B. \qquad (3.25\,d)$$

We transform the free-boundary problem (3.25) into fixed-domain problem via

$$y = \left(y_B - \frac{1}{2} \right) \zeta + \frac{1}{2}, \qquad (3.26)$$

where $\zeta \in [0, 1]$, which introduces the free-boundary coordinate as an explicit parameter in the system and then we add the trivial differential equation for the constant y_B to get the boundary value problem

$$\frac{1}{y_B - \frac{1}{2}} \partial_\zeta \left(\frac{\left(\frac{1}{y_B - \frac{1}{2}} \partial_\zeta N + \phi\, p_1 \right)(1 - \phi)}{\mathrm{Da}\,\phi^2} \right) = \frac{p_1 \left((y_B - \frac{1}{2})\zeta + \frac{1}{2} \right) + N}{1 - \phi} + \frac{1}{\eta_n} \qquad (3.27\,a)$$

$$\partial_\zeta y_B = 0 \qquad (3.27\,b)$$

with boundary conditions

$$0 = \partial_\zeta N + \left(y_b - \frac{1}{2} \right) \phi\, p_1 \qquad\qquad \text{at } \zeta = 0 \qquad (3.27\,c)$$

$$\phi = \phi_{sc} \qquad\qquad \text{at } \zeta = 1 \qquad (3.27\,d)$$

$$\partial_\zeta \phi = -\frac{2(y_b - \frac{1}{2})}{5(1 - \phi_{sc})} \frac{\mathrm{Da}^{\frac{1}{2}} \phi_{sc} (p_1 y_B + \mu_1)}{\tanh\left(\frac{\mathrm{Da}^{\frac{1}{2}} \phi_{sc}}{1 - \phi_{sc}} y_B \right)} + \frac{2}{5} \left(y_B - \frac{1}{2} \right) p_1 \qquad \text{at } \zeta = 1. \qquad (3.27\,e)$$

We have thus reduced our original system into a nonlinear boundary value problem, which can be solved using standard methods like Matlab's *bvp5c* solver.

After solving for ϕ, we can determine the remaining variables by first using (3.24) for w, next solving for $\phi_f \tau_{f12}$ via (3.16 *a*) with $(\phi_f \tau_{f12})(0) = 0$ and then get the fluid velocity via (3.16 *d*) with $u_f(1/2) = 0$. The solid variables are then easily computable by (3.16 *b*) and $u_s = u_f - w$.

3.1.2 *The minimum pressure condition*

We now derive a condition for the minimum pressure gradient that guaranties the existence of nontrivial solutions of the stationary problem.

Let y_{wall} be the position of the wall, i.e. in our case $y_{wall} = 1/2$, then the minimum magnitude for the pressure gradient $p_{\min}$ can be explicitly computed from (3.23 *b*) and
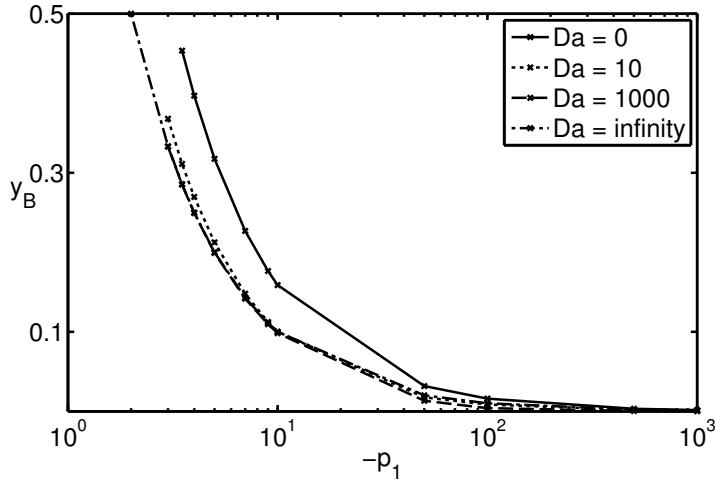
FIGURE 2. The dependence of the yield surface position y_B on the pressure gradient magnitude p_1, for parameters (3.31), $\mu_2 = 1$. The solid line shows the results for Da = 0; the dotted for Da = 10; the dashed curve for Da = 1000 and the dashed-dotted line for Da set to infinity.

$w(y_{wall}) = 0$ as

$$p_{\min} = \frac{\phi_{sc}\mathrm{Da}\mu_1}{y_{\mathrm{wall}}\phi_{sc}\mathrm{Da} + \sqrt{\mathrm{Da}}\tanh(\frac{y_{\mathrm{wall}}\sqrt{\mathrm{Da}}\phi_{sc}}{\phi_{sc}-1})(1 - \phi_{sc})^2}. \qquad (3.28)$$

This expression for $p_{\min}$ also contains the correct limits for infinite and zero Da when compared to (3.30) and (3.29). From this expression one can also see, that there must be always an unyielded region as $y_{\mathrm{wall}} \to 0$ implies $p_{\min} \to \infty$.

The dependence of the width of the unyielded zone on the pressure gradient is summarized in figure 2, for Da between 0 and infinity. In both cases, there is a minimum magnitude for the pressure gradient, i.e. p_{min}, below which the unyielded region fills the entire channel. On the other hand, as p_1 decreases, the width of the unyielded region decreases as well. In fact, y_B tends to zero as $p_1 \to -\infty$, but always remains strictly positive for finite pressure gradients. For larger Da the unyielded region is getting smaller and in the limit Da $\to \infty$ it becomes the curve

$$y_B = -\frac{\mu_1}{p_1}. \qquad (3.29)$$

For the other limit Da = 0 the yield surface position is

$$y_B = -\frac{\mu_1}{p_1\phi_{sc}}. \qquad (3.30)$$

Thus, we expect every y_B - p_1 - curve to be in between the two limits.

Problem (3.20 a), (3.20 b) with boundary conditions (3.16 f) and (3.23 b) contains the parameters Da, ϕ_{sc}, p_1, μ_1, μ_2, I_0. The critical volume fraction $\phi_{sc} \in [0.5; 0.74]$ is typically chosen as 0.5 (volume fraction at freezing point), 0.63 - 0.68 (volume fraction at maximum random packing) or 0.74 (volume fraction in a perfect crystal structure) depending on the application of interest. The channel pressure gradient value $p_1 \leq 0$ is a control parameter. Darcy's number Da is often given as the squared ratio of particle diameter,
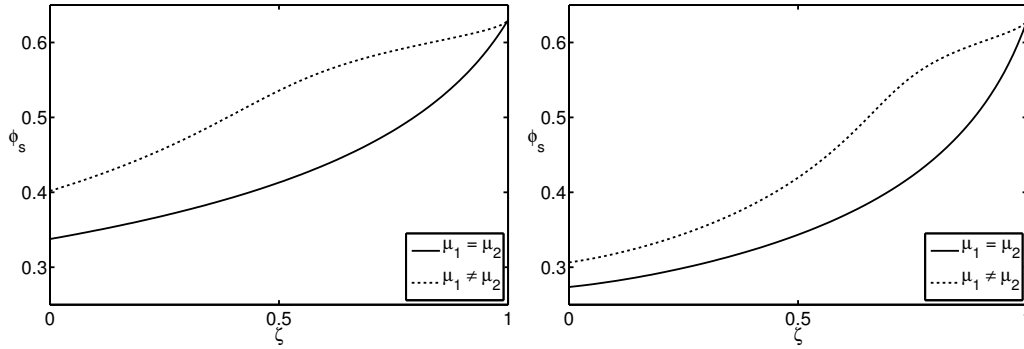
FIGURE 3. The trajectories for system (3.27), onto the ϕ_s-ζ-plane with $\mu_1 = \mu_2$ (continuous line) and $\mu_2 = 2$ (dotted line) as well as Da $= 1$ (left) and Da $= 1000$ (right).

i.e. Da $\approx (L/a)^2$, and can reach quite large values, see e.g. [25, 23]. The three parameter μ_1, μ_2 and I_0 are material parameters determined in [2] to be $\mu_1 = 0.32$, $\mu_2 = 0.7$ and $I_0 = 0.005$ by fitting to experimental data. In our study we fix

$$\phi_{sc} = 0.63, \qquad \mu_1 = 1, \qquad I_0 = 0.005, \tag{3.31}$$

and vary p_1 and Da for $\mu_1 = \mu_2$. Notice that in this case, the term that depends on I_0 drops out. After that, we let $\mu_2 = 1.5$ and again vary p_1 and Da. The reason we do not choose the values presented in [2] is an occurring instability for $\mu_1 < 1$ in the multiphase system as will be shown in a separate publication.

3.1.3 *Case $\mu_1 = \mu_2$*

Keeping in mind that we always keep the parameters in (3.31) fixed, we first consider $\mu_2 = \mu_1$ and let Da $= 1$ and $p_1 = -5$, shown in figure 3. If the magnitude of the pressure gradient is lowered below $p_{\min}$, the yield surface position y_B is at the wall, implying there is no yielded region and the unyielded region extends through the entire cross section of the channel. If, on the other hand, Da is raised to a large value, e.g. Da $= 1000$ with our first choice for the pressure gradient, the yield surface position becomes smaller, thus the unyielded region is thinner, as might have been expected for larger interphase stress due to drag. The effect in the $\phi_s - \zeta-$plane is a seemingly steeper ascent of the curve.

3.1.4 *Case $\mu_1 \neq \mu_2$*

Next, we consider $\mu_2 = 1.5 \neq \mu_1$ and Da $= 1$, $p_1 = -5$. The profile of ϕ is very similar to the $\mu_1 = \mu_2$ case, but it additionally contains an inflection point just before the volume fraction reaches the critical value ϕ_{sc}. This is a consequence of the second term in μ_c dominating the first term, i.e. μ_1 for ϕ_s close to the maximum packing fraction, provided $\mu_2 > \mu_1$ and $I_0 > 0$.

Summarizing, unless the absolute pressure gradient becomes smaller than $p_{\min}$, the results suggest that there always exists a unique solution to the boundary value problem (3.20).
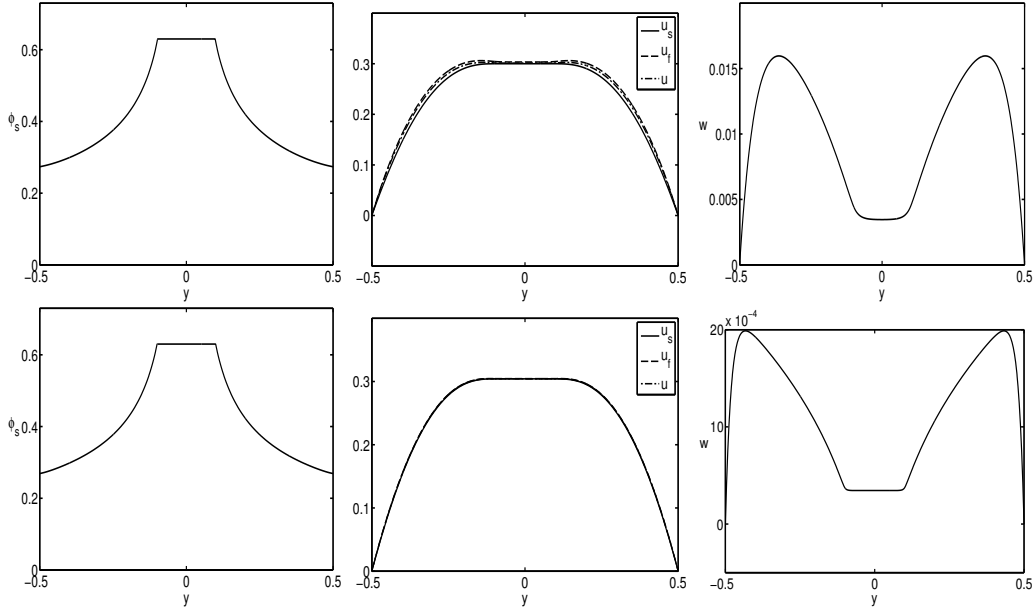
3.1.5 *Full solutions*

FIGURE 4. (left) The solid volume fraction ϕ_s, (middle) the velocities $\boldsymbol{u}_s, \boldsymbol{u}_f, \boldsymbol{u}$ and (right) the velocity difference w obtained by using the ODE problem (3.20). The parameters are given by (3.31), $\mu_2 = 1$, and $p_1 = -10$. Top figures show results for Da = 1000 and bottom figures for Da = 10000.

Figure 4 shows solutions for volume fraction, velocities and velocity difference across the whole channel. The solid volume fraction usually is increasing towards the channel center, where it has a non-vanishing region at maximum packing and falls back to its original value due to symmetry. The velocities are increasing towards the center, with a flattened profile around the unyielded region. We note that the fluid velocity has a dip around the center, thus reaches its maximum point not at the middle of the channel, but near the yield surface. The velocity difference w always has the form of a upside down w with a flattened region in the center.

We observe that for growing Da the solution of the stationary problem develops boundary layers, in particular the velocity w shows a pronounced sharp drop near the boundary $y = 1/2$. In the following section we will make use of this property to derive an asymptotic solution of the stationary problem in the limit Da $= 1/\varepsilon \to \infty$. We will expand on this analysis to derive a new drift-flux model from the time-dependent two-phase flow model for concentrated suspensions and use it to study the formation of unyielded or jammed regions in the flow.

3.2 Asymptotic analysis of the stationary state

For the typical physical situation we consider Da can become quite large and as we observed in the previous paragraph, at the same time the value of w becomes very small.

This suggest an asymptotic approximation of the problem using the ansatz

$$\mathrm{Da} = \frac{1}{\varepsilon}, \qquad w = \varepsilon \tilde{w}. \tag{3.32}$$

We denote in this paragraph $\phi \equiv \phi_s$ and also drop from now on the tilde. Then we have from $(3.20\,a)$-$(3.20\,b)$

$$w = p_1 \frac{1-\phi}{\phi} + \frac{1-\phi}{\phi^2} N'(\phi) \partial_y \phi. \tag{3.33\,a}$$

Substitution into equation for ϕ in $(3.20\,b)$ yield the second order equation for ϕ

$$\varepsilon \, \partial_y \left(p_1 \frac{1-\phi}{\phi} + \frac{1-\phi}{\phi^2} N'(\phi) \partial_y \phi \right) = \frac{p_1 y + N(\phi)}{1-\phi} + \frac{(\phi_{sc} - \phi)^2}{\phi^2}. \tag{3.33\,b}$$

The boundary conditions at the yield interface $y = y_B$ are

$$\phi = \phi_{sc}, \tag{3.33\,c}$$

$$\partial_y \phi = -\varepsilon^{-1/2} \frac{2}{5} \frac{\phi_{sc}}{1-\phi_{sc}} \frac{p_1 y_B + \mu_1}{\tanh\left(\frac{\phi_{sc}}{1-\phi_{sc}} \varepsilon^{-1/2} y_B \right)} + \frac{2}{5} p_1, \tag{3.33\,d}$$

and at the channel wall $y = \frac{1}{2}$ we have, since $w = 0$, so that $0 = p_1 \frac{1-\phi}{\phi} + \frac{1-\phi}{\phi^2} N'(\phi) \partial_y \phi$. Hence, we have the boundary condition

$$\partial_y \phi = -p_1 \frac{\phi}{N'(\phi)} \quad \text{at } y = \frac{1}{2}. \tag{3.33\,e}$$

Clearly, this is a singular perturbed problem with a boundary layer at $y = 1/2$ and $y = y_B$. In fact, if we assume that ϕ and y_B have asymptotic expansions

$$\phi(y) = \phi_0(y) + \varepsilon^{1/2} \phi_1(y) + O(\varepsilon), \qquad y_B = y_{B0} + \varepsilon \, y_{B1} + O(\varepsilon^2). \tag{3.34}$$

Then to leading order we have

$$0 = \frac{p_1 y + N(\phi_0)}{1-\phi_0} + \frac{(\phi_{sc} - \phi_0)^2}{\phi_0^2}. \tag{3.35}$$

When we use this in $(3.33\,a)$ the boundary conditions for w are not satisfied.

3.2.1 *Boundary layer problem at $y = 1/2$*

For the boundary layer variables $z = (\frac{1}{2} - y)\varepsilon^{-1/2}$ and $\Phi(z) = \phi(y)$ the governing equation is

$$\partial_z \left(-\varepsilon^{1/2} \, p_1 \frac{1-\Phi}{\Phi} + \frac{1-\Phi}{\Phi^2} N'(\Phi) \partial_z \Phi \right) = \frac{\frac{1}{2} p_1 + N(\Phi) - \varepsilon^{1/2} z}{1-\Phi} + \frac{(\phi_{sc} - \Phi)^2}{\Phi^2}, \tag{3.36\,a}$$

with boundary condition at $z = 0$

$$(1 - \Phi) \, N'(\Phi) \, \partial_z \Phi = \varepsilon^{1/2} \, p_1 \, (1 - \Phi)\Phi. \tag{3.36\,b}$$

Assume the asymptotic expansion of the inner variables can be written as

$$\Phi(z) = \Phi_0(z) + \varepsilon^{1/2} \Phi_1(z) + O(\varepsilon), \tag{3.37}$$

so that the solution satisfies to leading order the problem

$$\partial_z \left(\frac{1 - \Phi_0}{\Phi_0^2} \, N'(\Phi_0) \, \partial_z \Phi_0 \right) = \frac{\frac{1}{2} p_1 + N(\Phi_0)}{1 - \Phi_0} + \frac{(\phi_{sc} - \Phi_0)^2}{\Phi_0^2} \tag{3.38 a}$$

$$\partial_z \Phi_0 = 0 \qquad \text{at} \quad z = 0^+ \tag{3.38 b}$$

since $(1 - \Phi_0) \, N'(\Phi_0) \neq 0$. As $z \to \infty$ the solution approaches a constant, say $\Phi_0 \to \Phi_{0,\infty}$, which satisfies

$$\frac{\frac{1}{2} \, p_1 + N(\Phi_{0,\infty})}{1 - \Phi_{0,\infty}} + \frac{(\phi_{sc} - \Phi_{0,\infty})^2}{\Phi_{0,\infty}^2} = 0. \tag{3.39}$$

Hence, since for $y \to (1/2)^-$ in the leading order outer problem, then

$$0 = \frac{\frac{1}{2} \, p_1 + N\left(\phi_0(\frac{1}{2})\right)}{1 - \phi_0(\frac{1}{2})} + \frac{\left(\phi_{sc} - \phi_0(\frac{1}{2})\right)^2}{\phi_0^2(\frac{1}{2})}. \tag{3.40}$$

Therefore, matching yields $\Phi_{0,\infty} = \phi_0(1/2)$.

It is straightforward to solve the next order problem to obtain

$$\Phi_1(z) = \frac{A_2 N'(\phi_0\,(1/2)) - p_1 \phi_0\,(1/2)\, A_1}{A_1^{3/2} N'(\phi_0\,(1/2))} \exp\left(-\sqrt{A_1} z\right) + \frac{A_2}{A_1} z, \tag{3.41}$$

where

$$A_1 = \frac{\phi_0^2\,(1/2)}{(1 - \phi_0\,(1/2))^2} + \frac{\phi_0^2\,(1/2)}{N'(\phi_0\,(1/2))} \frac{\frac{1}{2} p_1 + N(\phi_0\,(1/2))}{(1 - \phi_0\,(1/2))^3}$$

$$- \frac{2}{N'(\phi_0\,(1/2))} \frac{\phi_{sc}}{\phi_0\,(1/2)} \frac{\phi_{sc} - \phi_0\,(1/2)}{1 - \phi_0\,(1/2)}, \tag{3.42 a}$$

$$A_2 = \frac{p_1}{N'(\phi_0\,(1/2))} \frac{\phi_0^2\,(1/2)}{(1 - \phi_0\,(1/2))^2}, \tag{3.42 b}$$

thus, using (3.40)

$$\frac{A_2}{A_1} = p_1 \left[N'(\phi_0\,(1/2)) + \frac{(\phi_{sc} - \phi_0\,(1/2)) \left(\phi_0^2\,(1/2) - 2\phi_{sc} + \phi_{sc}\phi_0\,(1/2)\right)}{\phi_0^3\,(1/2)} \right]^{-1}. \tag{3.43}$$

Taking the y-derivative of (3.35) we get

$$\partial_y \phi_0 = -p_1 \left[N'(\phi_0) + \frac{\phi_{sc} - \phi_0}{\phi_0^3} \left(\phi_0^2 - 2\phi_{sc} + \phi_0\phi_{sc}\right) \right]^{-1}. \tag{3.44}$$

Therefore, the linear term in the expansion of the outer solution ϕ_0 and in the inner solution Φ_1, see (3.41), match as required.

3.2.2 Boundary layer problem at $y = y_B$

Similarly, we let the boundary layer variables be

$$\xi = \frac{y - y_B}{\varepsilon^{1/2}}, \qquad \varphi(\xi) = \phi(y). \tag{3.45}$$

To leading order the problem now reads

$$\partial_\xi \left(\frac{1 - \varphi_0}{\varphi_0^2} \, N'(\varphi_0) \, \partial_\xi \varphi_0 \right) = \frac{p_1 \, y_{B0} + N(\varphi_0)}{1 - \varphi_0} + \frac{(\phi_{sc} - \varphi_0)^2}{\varphi_0^2}, \tag{3.46 a}$$

with boundary condition at $\xi = 0^+$

$$\varphi_0(0) = \phi_{sc} \qquad (3.46\,b)$$

and

$$\partial_\xi \varphi_0(0) = -\frac{2}{5} \frac{\phi_{sc}}{1 - \phi_{sc}} \left(p_1 \, y_{B0} + \mu_1\right) = 0. \qquad (3.46\,c)$$

Note, if we assume that in the leading order outer equation, ϕ also satisfies $\phi = \phi_{sc}$ at $y = y_B$ then we must have that $p_1 \, y_{B0} + \mu_1 = 0$, since $N(\phi_{sc}) = \mu_1$. Hence, the second boundary condition is also zero. This suggests $\varphi_0 = \phi_{sc}$. Matching this to the leading order outer problem

$$\frac{p_1 \, y_{B0} + N(\phi_0(y_{B0}))}{1 - \phi_0(y_B)} + \frac{(\phi_{sc} - \phi_0(y_B))^2}{\phi_0^2(y_B)} = 0. \qquad (3.47)$$

Hence, $\phi_0(y_B) = \phi_{sc}$. Solving the next order problem

$$\partial_{\xi\xi} \varphi_1 = \left(\varphi_1 - \frac{2}{5} p_1 \xi\right) \frac{\phi_{sc}^2}{(1 - \phi_{sc})^2} \qquad (3.48\,a)$$

with boundary conditions

$$\varphi_1(0) = 0, \quad \partial_\xi \varphi_1(0) = \frac{2}{5} p_1 \qquad (3.48\,b)$$

gives

$$\varphi_1(\xi) = \frac{2}{5} p_1 \xi. \qquad (3.49)$$

This needs to be matched with the linear term in the Taylor expansion of the leading order outer solution ϕ_0, which can be obtained by taking the limit $\phi \to \phi_{sc}$ in (3.44). That limit gives $\partial_y \phi_0(y_B) = -p_1/N'(\phi_{sc}) = -p_1/(-5/2)$, that is, the coefficients are equal, hence the terms match.

Higher order approximations, that include the perturbation of the boundary will only come in at $O(\varepsilon)$ and are not considered here.

4 Drift-flux model for plane Poiseuille flow

Drift-flux models are well-known and have been proposed to study the evolution of two-phase flows of suspensions [20, 26]. They are also used as transport equations for a suspended phase and combined with hydrodynamic equations [7, 24]. Here we will use matched asymptotics along the lines of the analysis of the stationary problem, for the derivation of a new drift-flux model for the cross-section of the channel. Our analysis shows that the inclusion of the boundary layers leads to a drift-flux model that naturally accounts for the shear-induced flux of the suspended phase away from the boundaries. Moreover, the constitutive law for concentrated suspensions leads to the appearance of unyielded and yielded regions, which needs to be captured by the new drift-flux model.

4.1 Asymptotic model

To capture the evolution towards a Bingham-type flow it will be instructive to investigate the problem for the cross-section. We assume therefore that all the variables depend only

on y and t, except for the pressure variables, which depend in addition on x. As in our previous section, the drift-flux regime is established for large Da and small velocity differences w, and in addition on a long time scale. Hence we let

$$\mathrm{Da} = \frac{1}{\varepsilon}, \quad w_1 = \varepsilon w_1^*, \quad w_2 = \varepsilon w_2^*, \quad t = \frac{t^*}{\varepsilon}. \tag{4.1}$$

The governing equations are then, after we drop the "$*$"

$$\partial_t \phi - \partial_y(\phi(1-\phi)w_2) = 0 \tag{4.2 a}$$

$$-\partial_y\left[(1-\phi)\,\partial_y v_1 + \varepsilon(1-\phi)\,\partial_y(\phi w_1)\right] + (1-\phi)\partial_x p_f = -\frac{\phi^2}{1-\phi}w_1 \tag{4.2 b}$$

$$-\partial_y\left[2\varepsilon(1-\phi)\,\partial_y(\phi w_2)\right] + (1-\phi)\partial_y p_f = -\frac{\phi^2}{1-\phi}w_2 \tag{4.2 c}$$

$$-\partial_y\left[\phi\eta_s\partial_y v_1 - \varepsilon\phi\eta_s\partial_y((1-\phi)w_1)\right] + \phi\partial_x p_f = \frac{\phi^2}{1-\phi}w_1 \tag{4.2 d}$$

$$\partial_y\left[2\varepsilon\phi\,\partial_y((1-\phi)w_2)\right] + \phi_s\partial_y p_f + \partial_y p_c = \frac{\phi^2}{1-\phi}w_2 \tag{4.2 e}$$

$$p_c = \eta_n(\phi)\left[(\partial_y v_1 - \varepsilon\partial_y((1-\phi)w_1))^2 + 2\varepsilon[\partial_y((1-\phi)w_2)]^2\right]^{1/2} \tag{4.2 f}$$

and no-slip conditions at $y = \pm 1/2$

$$v_1 = 0, \quad w_1 = 0, \quad w_2 = 0. \tag{4.2 g}$$

To leading order we obtain for the outer problem

$$\partial_t \phi - \partial_y(\phi(1-\phi)w_2) = 0 \tag{4.3 a}$$

$$-\partial_y[(1-\phi)\partial_y v_1] + (1-\phi)\partial_x p_f = -\frac{\phi^2}{1-\phi}w_1 \tag{4.3 b}$$

$$(1-\phi)\partial_y p_f = -\frac{\phi^2}{1-\phi}w_2 \tag{4.3 c}$$

$$-\partial_y[\phi\eta_s\partial_y v_1] + \phi\partial_x p_f + \partial_x p_c = \frac{\phi^2}{1-\phi}w_1 \tag{4.3 d}$$

$$\phi\partial_y p_f + \partial_y p_c = \frac{\phi^2}{1-\phi}w_2 \tag{4.3 e}$$

$$p_c = \eta_n \left|\partial_y v_1\right|, \tag{4.3 f}$$

and no-slip conditions at $y = \pm 1/2$

$$v_1 = 0, \quad w_1 = 0, \quad w_2 = 0. \tag{4.3 g}$$

We note that for ease of notation we have dropped the indices in the variables that denote the leading order solutions. Adding (4.3 c) and (4.3 e) yields $\partial_y(p_f + p_c) = 0$, hence $p_f + p_c = f(x)$. Adding (4.3 b) and (4.3 d) yields

$$-\partial_y\left([\phi\eta_s + (1-\phi)]\,\partial_y v_1\right) + \partial_x(p_f + p_c) = 0. \tag{4.4}$$

Since the left hand side is only dependent on y and the right hand side only on x, they

must be constants. Thus, defining $\partial_x(p_f + p_c) = p_1$, so that after integration

$$[\phi\eta_s + (1 - \phi)]\,\partial_y v_1 = p_1 y + \alpha. \tag{4.5}$$

Adding $(1 - \phi)\partial_y p_c$ on both sides of $(4.3\,c)$ yields

$$\partial_y p_c = \frac{\phi^2}{(1 - \phi)^2}w_2. \tag{4.6}$$

We have

$$w_2 = \frac{(1 - \phi)^2}{\phi^2}\partial_y\left(\eta_n|\partial_y v_1|\right) = \frac{(1 - \phi)^2}{\phi^2}\partial_y\left(\eta_n\dot{\gamma}\right). \tag{4.7}$$

In addition note that from (4.5) we obtain

$$\partial_y v_1 = \frac{p_1\,y}{\phi\eta_s + 1 - \phi}, \tag{4.8}$$

where due to symmetry we have set $\alpha = 0$. Since $p_1 < 0$ the negative of this expression will always be positive and we set

$$\dot{\gamma} = -\frac{p_1\,y}{\phi\eta_s + 1 - \phi}, \tag{4.9}$$

so that

$$w_2 = -p_1\frac{(1 - \phi)^2}{\phi^2}\partial_y\left[\frac{\eta_n y}{\phi\eta_s + 1 - \phi}\right]. \tag{4.10}$$

Hence, we obtain for the drift-flux model

$$\partial_t\phi = -p_1\partial_y\left[\frac{(1 - \phi)^3}{\phi}\partial_y\left(\frac{y}{N(\phi) + \frac{1 - \phi}{\eta_n(\phi)}}\right)\right]. \tag{4.11}$$

We note at this point that the drift-flux model we have just derived (4.11) is a nonlinear diffusion equation which admits constant solutions, say ϕ_0. Linearizing about these base states by making the ansatz $\phi(t, y) = \phi_0 + \delta\,\phi_1(t, y) + O(\delta^2)$ we obtain to $O(\delta)$

$$\partial_t\phi_1 = -p_1\,\partial_y\left[\frac{M'(\phi_0)}{K(\phi_0)}\phi_1 - M(\phi_0)\frac{K'(\phi_0)}{K^2(\phi_0)}\partial_y\left(y\phi_1\right)\right], \tag{4.12}$$

where $M(\phi) = (1 - \phi)^3/\phi$ and $K(\phi) = N(\phi) + (1 - \phi)/\eta_n(\phi)$. Clearly, if $K'(\phi_0) < 0$ then any perturbation of the constant bases states will be damped out and the flow will remain constant. But we note that constant solutions will not satisfy the boundary conditions unless the constant is zero. Hence we expect the nonlinear structure to come from the interplay between the drift-flux equation and the no-flux condition.

We now supplement this equation with boundary conditions. At the wall, $y = 1/2$, it seems plausible to use no-flux conditions, and indeed, matching to a boundary layer there gives $w_2 = 0$, see appendix C. We seek solutions that are symmetric with respect to the middle axis of the channel, thus we also impose $w_2 = 0$ at $y = 0$.

We expect that the flux of the solid phase will lead to an increase of ϕ at the centre of the channel. At some time, in fact, the solid volume fraction will reach ϕ_{sc} there and jamming will occur. After that, flow of both phases will only occur for $y > y_B$, while for $y < y_B$, the solid phase will be jammed, where y_B is a time dependent free boundary. In this region, the volume fractions are constant so that the mass conservation equations

give $w_2 = w_2(t)$. Assuming symmetry at $y = 0$ then fixes w_2 to be zero to all orders in ε for $0 < y < y_B$. At $y = y_B$, we therefore impose $\phi = \phi_{sc}$ and $w_2 = 0$, so that we have two boundary conditions as required at a free boundary.

Remark

We remark that in the stationary case we let $\partial_t \phi = 0$ in (4.11), and integrate once. Using the condition that $\bar{w}_2 = 0$ at the channel walls, the integration constant must be zero. Since $(1 - \phi)^3/\phi$ will never be zero, we can divide and integrate once more to obtain

$$\frac{y}{N(\phi) + \frac{1-\phi}{\eta_n(\phi)}} = c. \tag{4.13}$$

With $c = -1/p_1$ we obtain the stationary outer equation (3.35).

4.2 Numerical solution of the drift-flux model

In order to understand the time evolution of the solid volume fraction in a channel, we numerical solve (4.11) with no-flux boundary conditions

$$\partial_y \left(\frac{y}{N(\phi) + \frac{1-\phi}{\eta_n(\phi)}} \right) = 0 \qquad \text{at } y \in \left\{ y_B, \frac{1}{2} \right\} \tag{4.14}$$

using a central finite difference scheme of second order with a fully implicit Euler-Euler-2-step method. The free-boundary condition

$$\phi = \phi_{sc} \quad \text{at } y = y_B \tag{4.15}$$

is used to update the position of the yield surface y_B.

The time evolution is shown in figure 5 for the parameters from (3.31) with $\mu_1 = \mu_2$ and $p_1 = -10$, starting from an initial uniform profile of $\phi(0, y) = \frac{1}{2}\phi_{sc}$. The profile first changes near the channel center and wall. Next, the volume fraction increases near the center until maximum packing is reached, which spawns an unyielded region. This unyielded region then grows until the yield surface y_B reaches the value from (3.29), where the evolution stops as the stationary solution is reached.

The stationary profile obtained by the drift-flux model has the same parameters $\mu_1, \mu_2, I_0, \phi_{sc}, \text{Da}$, but not p_1. The pressure p_1 must then be chosen, so that the volume of solids V_s in a cross section of the channel is matching, i.e.

$$V_s(t) = \int_{-1/2}^{1/2} \phi(t, y) \, \mathrm{d}y \tag{4.16}$$

must be the same for the stationary and the drift-flux solution. A simple way achieving this is to measure the yield surface position y_B and use equation (3.29) for the pressure of the stationary solution.
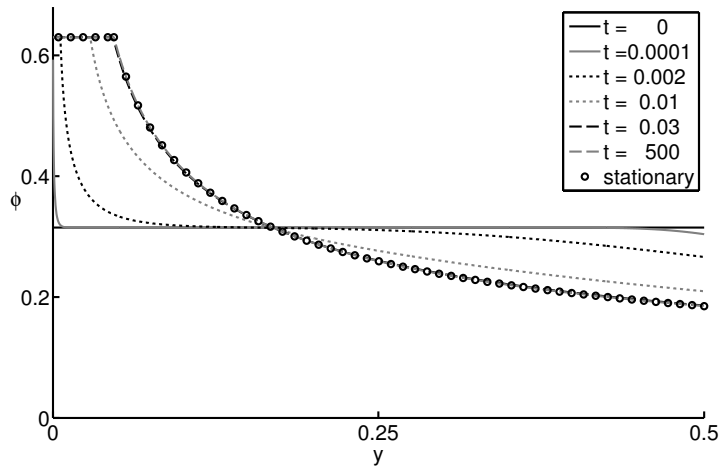
FIGURE 5. Time evolution of solid volume fraction using the outer drift-flux approximation (4.11).

5 Conclusion and Outlook

In this study we presented the derivation of a new drift-flux model using matched asymptotic expansions, for concentrated non-Brownian suspensions that allow for the emergence of jammed regions. We showed how the underlying two-phase model itself can be systematically derived through ensemble averaging along the lines of Drew et al. [11] while incorporating recent constitutive laws by Boyer et al. [2] for the shear and normal viscosities for concentrated suspensions.

Our study of plane Poiseuille flow using the two-phase model shows the existence of unyielded or jammed regions. The emergence of such a region and its width depend critically on the value of the applied pressure for given volume fraction of the solid phase. We also demonstrated the dependence of the profile for the volume fraction ϕ_s on the so-called "viscous number", which can induce a qualitative change in the approach towards maximum volume fraction. Interestingly, for the typically large values of Da the flow variable $w_1 = u_f - u_s$, i.e. the difference between the velocities of the fluid phase u_f and the solid phase u_s develops a boundary layer at the channel walls and at the interface between unyielded and yielded regions.

Our asymptotic analysis, which we generalized for the time-dependent problem, shows that in order for the drift-flux model to correctly capture shear-induced particle migration the boundary layer structure of the solution has to be resolved and matched to the "outer" problem of the drift-flux model.

We then showed numerically how the flow pattern emerges in time once the boundary layer at the channel walls are established and show the slow approach towards the stationary solution of the two-phase model. It would be interesting to compare this evolution to experimental results on a transition length towards the steady state in the future.

Our analysis suggests that the boundary layer acts as a source for the particle migration towards the unyielded region. Our asymptotic analysis shows that the quantities w_1, w_2, which denote the difference between the velocities u_f, u_s and v_f, v_s, respectively,

are by $O(\varepsilon)$ smaller than the actual flow variables. The fact that the particle transport acts on a different asymptotic scale than the actual flow field also suggests how to systematically develop an asymptotic theory leading to a complete coupled flow model that includes transport and even jamming of particles. In some way such an analysis could also rationalize some of the suspension flow models that are found in the literature. In fact, using the methods presented in this study should also enable the systematic derivation of drift-flux models for more complex flow geometries, including for example a free boundary between the suspension and the surrounding atmosphere, and will be part of our future work.

Appendix A Averaging rules

We will follow the mathematical framework by Drew and Passman [9],[10] in this section. Let f and g be arbitrary measurable functions, c a constant and $\langle \cdot \rangle$ an average operator obeying the so-called Reynolds' rules

$$\langle f + g \rangle = \langle f \rangle + \langle g \rangle \tag{A 1}$$

$$\langle \langle f \rangle g \rangle = \langle f \rangle \langle g \rangle \tag{A 2}$$

$$\langle c \rangle = c, \tag{A 3}$$

the Leibniz' rule

$$\langle \partial_t f \rangle = \partial_t \langle f \rangle \tag{A 4}$$

and the Gauss' rule

$$\langle \partial_i f \rangle = \partial_i \langle f \rangle. \tag{A 5}$$

The functions should be weakly differentiable up to the required order. Admissible operators are for example the volume average [31], [19], time averages [17], the ensemble average [10] or a mixture of these [11]. However, note the derivatives are defined in the sense of distributions in this work. This implies $\langle \nabla f \rangle$ can have a Dirac delta property yielding additional surface integrals, whereas in classical theories the Leibniz' and Gauss' rule are written explicitly with surface integrals, c.f. [10] and [31].

We further need a component indicator function

$$X_k(\boldsymbol{x}, t) = \begin{cases} 1, & \text{if } (\boldsymbol{x}, t) \in K \\ 0, & \text{if } (\boldsymbol{x}, t) \notin K \end{cases} \tag{A 6}$$

with K the set of states of the k-th-phase. In our model we use the average operator in a

weighted form. There are in general two averages in use, the intrinsic or phasic average

$$\overline{g} \equiv \frac{\langle X_k g \rangle}{\langle X_k \rangle} \tag{A7}$$

and the mass-weighted or Favré average (in its three common forms)

$$\widehat{g} \equiv \frac{\overline{\rho g}}{\overline{\rho}} = \frac{\langle X_k \rho g \rangle}{\langle X_k \rangle \frac{\langle X_k \rho \rangle}{\langle X_k \rangle}} = \frac{\langle X_k \rho g \rangle}{\langle X_k \rho \rangle}. \tag{A8}$$

When we have multiple indicator functions, an index states the indicator function we used in the average, e.g. $\overline{g}_s$ means we used X_s in the average. We define a fluctuation field (cf. [10]) as

$$g' := g - \overline{g} \tag{A9}$$

$$g^\circ := g - \widehat{g} \tag{A10}$$

and due to the Reynolds rules $\overline{g'} = \widehat{g^\circ} = 0$ holds. This splitting together with the Reynolds rules yields the identity

$$\overline{fg} = \overline{f}\,\overline{g} + \overline{f'g'} \tag{A11}$$

and similar for the Favré average

$$\widehat{fg} = \widehat{f}\widehat{g} + \widehat{f^\circ g^\circ}. \tag{A12}$$

The characteristic function fulfills the so-called topological equation (cf. [10])

$$\partial_t X_k + \boldsymbol{u}_i \cdot \nabla X_k = 0 \tag{A13}$$

with $\boldsymbol{u}_i$ the interface velocity.

Appendix B Derivation of the two-phase flow model

As in [10] we introduce the component indicator function

$$X_k(\boldsymbol{x}, t) = \begin{cases} 1, & \text{if } (\boldsymbol{x}, t) \in K, \\ 0, & \text{if } (\boldsymbol{x}, t) \notin K. \end{cases} \tag{B1}$$

We further define an average operator $\langle \cdot \rangle$ obeying the so-called Reynolds' rules, the Leibniz' rule and the Gauss' rule, which are given in the appendix A.

We further define an average operator $\langle \cdot \rangle$ obeying the so-called Reynolds' rules, the Leibniz' rule and the Gauss' rule, which are given in the appendix A.

Multiplication with X_k, followed by usage of the average operator and its linearity together with Gauss' and Leibniz' rules yield

$$\partial_t \langle X_k \rho \rangle + \nabla \cdot \langle X_k \rho \boldsymbol{u} \rangle = \langle \rho(\partial_t X_k + \boldsymbol{u}_i \nabla \cdot X_k) \rangle \tag{B2}$$

$$+ \langle \rho(\boldsymbol{u} - \boldsymbol{u}_i) \cdot \nabla X_k \rangle \tag{B3}$$

$$\partial_t \langle X_k \rho \boldsymbol{u} \rangle + \nabla \cdot \langle X_k \rho \boldsymbol{u} \otimes \boldsymbol{u} \rangle - \nabla \cdot \langle X_k \boldsymbol{T} \rangle = \langle X_k \boldsymbol{f} \rangle \tag{B4}$$

$$+ \langle (\partial_t X_k + \boldsymbol{u}_i \cdot \nabla X_k) \rho \boldsymbol{u} \rangle \tag{B5}$$

$$+ \langle [(\boldsymbol{u} - \boldsymbol{u}_i) \cdot \nabla X_k] \rho \boldsymbol{u} \rangle - \langle \nabla X_k \cdot \boldsymbol{T} \rangle. \tag{B6}$$

In the above we assume that the interface velocity $\boldsymbol{u}_i$ has been smoothly extended for all x. Since the indicator function satisfies the so-called topological equation (cf. [10])

$$\partial_t X_k + \boldsymbol{u}_i \cdot \nabla X_k = 0, \tag{B 7}$$

the first and the second term equations (B 2) and (B 5) drop out, respectively, and we can write the system as

$$\partial_t \langle X_k \rho \rangle + \nabla \cdot \langle X_k \rho \boldsymbol{u} \rangle = \boldsymbol{\Gamma}_k \tag{B 8}$$

$$\partial_t \langle X_k \rho \boldsymbol{u} \rangle + \nabla \cdot \langle X_k \rho \boldsymbol{u} \otimes \boldsymbol{u} \rangle \tag{B 9}$$

$$-\nabla \cdot \langle X_k \boldsymbol{T} \rangle = \langle X_k \boldsymbol{f} \rangle + \boldsymbol{M}_k, \tag{B 10}$$

where

$$\boldsymbol{\Gamma}_k \equiv \langle \rho(\boldsymbol{u} - \boldsymbol{u}_i) \cdot \nabla X_k \rangle, \tag{B 11}$$

$$\boldsymbol{M}_k \equiv \langle \nabla X_k \cdot [\rho(\boldsymbol{u} - \boldsymbol{u}_i) \otimes \boldsymbol{u} - \boldsymbol{T}] \rangle, \tag{B 12}$$

denotes the average interfacial mass source and the average interfacial momentum source for the k-th phase, respectively.

To obtain the averaged form of the jump conditions, we note first the Dirac delta property of the component indicator functions' derivative

$$\langle \nabla X_k f \rangle = -\int_{\mathcal{S}_k} \boldsymbol{n}_k f_k d\boldsymbol{S}, \tag{B 13}$$

with $\mathcal{S}_k$ the interface of phase k. Using this and (B 11), (B 12) in the jump conditions for mass (2.3) and momentum (2.4), these conditions become

$$\sum_k \boldsymbol{\Gamma}_k = 0, \tag{B 14}$$

$$\sum_k \boldsymbol{M}_k = \langle \sigma_{fs} \kappa \nabla X_1 \rangle. \tag{B 15}$$

We further introduce the following averaged quantities (for notation see appendix A)

$$\phi_k \equiv \langle X_k \rangle,$$

for the volume fraction, and

$$\overline{\rho}_k \equiv \frac{\langle X_k \rho \rangle}{\phi_k},$$

$$\widehat{\boldsymbol{u}}_k \equiv \frac{\langle X_k \rho \boldsymbol{u} \rangle}{\phi_k \overline{\rho}_k},$$

$$\overline{\boldsymbol{T}}_k \equiv -\frac{\langle X_k \boldsymbol{T} \rangle}{\phi_k},$$

$$\boldsymbol{T}_k^{Re} \equiv -\frac{\langle X_k \rho \boldsymbol{u}_k^\circ \otimes \boldsymbol{u}_k^\circ \rangle}{\phi_k},$$

$$\overline{\boldsymbol{f}}_k \equiv \frac{\langle X_k \boldsymbol{f} \rangle}{\phi_k},$$

$$\boldsymbol{S}_k^d \equiv -\langle \nabla X_k \cdot \boldsymbol{T} \rangle,$$

$$\overline{\boldsymbol{u}}_{ki} \boldsymbol{\Gamma}_k \equiv \langle \nabla X_k \cdot \rho (\boldsymbol{u} - \boldsymbol{u}_i) \otimes \boldsymbol{u} \rangle$$

for the average density, velocity, stress, Reynolds stress, body forces, interfacial stress, interfacial velocity of the kth phase, respectively.

Then, after we split the interfacial momentum source as

$$\boldsymbol{M}_k = \boldsymbol{S}_k^d + \overline{\boldsymbol{u}}_{ki} \boldsymbol{\Gamma}_k \tag{B 16}$$

and the momentum flux into an average flux and a Reynolds stress

$$\langle X_k \rho \boldsymbol{u} \otimes \boldsymbol{u} \rangle = \phi_k \overline{\rho}_k \widehat{\boldsymbol{u}}_k \otimes \widehat{\boldsymbol{u}}_k - \phi_k \boldsymbol{T}_k^{Re}, \tag{B 17}$$

and use the product rule (A 12) for the velocity, we obtain the following system of phase averaged mass and momentum equations

$$\partial_t(\phi_k \overline{\rho}_k) + \nabla \cdot (\phi_k \overline{\rho}_k \widehat{\boldsymbol{u}}_k) = \boldsymbol{\Gamma}_k, \tag{B 18}$$

$$\partial_t(\phi_k \overline{\rho}_k \widehat{\boldsymbol{u}}_k) + \nabla \cdot (\phi_k \overline{\rho}_k \widehat{\boldsymbol{u}}_k \otimes \widehat{\boldsymbol{u}}_k) - \nabla \cdot (\phi_k \overline{\boldsymbol{T}}_k) = \tag{B 19}$$

$$\nabla \cdot (\phi_k \boldsymbol{T}_k^{Re}) + \overline{\boldsymbol{f}}_k + \boldsymbol{S}_k^d + \overline{\boldsymbol{u}}_{ki} \boldsymbol{\Gamma}_k. \tag{B 20}$$

As we are interested in the laminar flow regime we neglect the Reynolds stress $\boldsymbol{T}_k^{Re}$ and further assume no phase change occurs at the interface between particles and liquid, $\boldsymbol{\Gamma}_k = 0$.

We introduce the stress tensor as the sum of pressure and deviatoric stress in the form

$$\boldsymbol{T} = -p\boldsymbol{I} + \boldsymbol{\tau}, \tag{B 21}$$

so that for the averaged quantities $\overline{\boldsymbol{T}}_k$ and

$$\overline{p}_k \equiv \frac{\langle X_k p \rangle}{\phi_k}, \tag{B 22}$$

$$\overline{\boldsymbol{\tau}}_k \equiv -\frac{\langle X_k \boldsymbol{\tau} \rangle}{\phi_k}, \tag{B 23}$$

we have correspondingly

$$\overline{\boldsymbol{T}}_k = -\overline{p}_k \boldsymbol{I} + \overline{\boldsymbol{\tau}}_k. \tag{B 24}$$

The interfacial pressure of phase k and the interfacial force density is defined as

$$\tilde{p}_{ik} \equiv \frac{\langle \nabla X_k p_k \rangle}{\langle \nabla X_k \rangle} = \frac{\langle \nabla X_k p_k \rangle}{\nabla \phi_k}, \tag{B 25}$$

$$\boldsymbol{M}_k^d \equiv \boldsymbol{S}_k^d - \langle \nabla X_k p_k \rangle = \langle \nabla X_k \cdot ((p_k - \tilde{p}_{ik})\boldsymbol{I} - \boldsymbol{\tau}) \rangle, \tag{B 26}$$

respectively, where the second equality in (B 25) follows from an application of Gauss' rule (A 5). We have (from (B 16))

$$\boldsymbol{M}_k = \boldsymbol{M}_k^d + \tilde{p}_{ik} \nabla \phi_k, \tag{B 27}$$

so that we obtain for the mass and momentum balance equations

$$\partial_t(\phi_k \overline{\rho}_k) + \nabla \cdot (\phi_k \overline{\rho}_k \widehat{\boldsymbol{u}}_k) = 0, \tag{B 28}$$

$$\partial_t(\phi_k \overline{\rho}_k \widehat{\boldsymbol{u}}_k) + \nabla \cdot (\phi_k \overline{\rho}_k \widehat{\boldsymbol{u}}_k \otimes \widehat{\boldsymbol{u}}_k) \tag{B 29}$$

$$- \nabla \cdot (\phi_k \overline{\boldsymbol{\tau}}_k) + \nabla(\phi_k \overline{p}_k) = \boldsymbol{M}_k^d + \tilde{p}_{ik} \nabla \phi_k, \tag{B 30}$$

where we have also assumed that no external body forces are applied, i.e. $\overline{\boldsymbol{f}} = 0$.

We neglect surface tension forces between the solid and the liquid phase [9]. Setting $\sigma_{fs} = 0$ the interfacial pressure difference becomes

$$\sum_k \tilde{p}_{ik} \nabla \phi_k = \langle \sigma \kappa \nabla X_s \rangle = 0, \tag{B 31}$$

and we obtain together with the interfacial momentum jump condition (B 15) the relation

$$M_s^d = -M_f^d. \tag{B 32}$$

Since we only have two phases, we know $\phi_s + \phi_f = 1$, which directly leads to $\nabla \phi_s = -\nabla \phi_f$. Thus, equation (B 31) yields

$$\tilde{p}_{is} = \tilde{p}_{if}.$$

For the case of identical liquid interfacial and bulk pressure

$$\tilde{p}_{if} = \overline{p}_f,$$

and constant densities $\overline{\rho}_k$ within each phase, the balance equations reduce to the system (2.6) in the text.

Appendix C Boundary layer analysis for the drift-flux model

For the boundary layer analysis at the wall we introduce variable

$$z = \frac{\frac{1}{2} - y}{\varepsilon^{1/2}}, \qquad \Phi(t, z) = \phi_s(t, y) = \phi(t, y). \tag{C 1}$$

Then we obtain

$$\varepsilon^{1/2}\partial_t\Phi + \partial_z(\Phi(1-\Phi)w_2) = 0 \qquad (C\,2\,a)$$

$$-\partial_z\left[(1-\Phi)\partial_z v_1 + \varepsilon(1-\Phi)\partial_z(\Phi w_1)\right] + \varepsilon(1-\Phi)\partial_x p_f = -\varepsilon\frac{\Phi^2}{1-\Phi}w_1 \qquad (C\,2\,b)$$

$$\varepsilon^{1/2}\partial_z\left[2(1-\Phi)\partial_z(\Phi w_2)\right] + (1-\Phi)\partial_z p_f = \varepsilon^{1/2}\frac{\Phi^2}{1-\Phi}w_2 \qquad (C\,2\,c)$$

$$-\partial_z\left[\Phi\eta_s\partial_z v_1 - \varepsilon\Phi\eta_s\partial_z((1-\Phi)w_1)\right] + \varepsilon\Phi\partial_x p_f = \varepsilon\frac{\Phi^2}{1-\Phi}w_1 \qquad (C\,2\,d)$$

$$\varepsilon^{1/2}\partial_z\left[2\Phi\partial_z((1-\Phi)w_2)\right] - \Phi\partial_z p_f - \partial_z p_c = \varepsilon^{1/2}\frac{\Phi^2}{1-\Phi}w_2 \qquad (C\,2\,e)$$

and

$$p_c = \eta_n\left[\frac{1}{\varepsilon}(\partial_z v_1 - \varepsilon\partial_z((1-\Phi)w_1))^2 + 2[\partial_z((1-\Phi)w_2)]^2\right]^{1/2} \qquad (C\,2\,f)$$

and no-slip conditions at $z = 0$

$$v_1 = 0, \quad w_1 = 0, \quad w_2 = 0. \qquad (C\,2\,g)$$

The leading order system is

$$\partial_z(\Phi(1-\Phi)w_2) = 0 \qquad (C\,3\,a)$$
$$-\partial_z\left[(1-\Phi)\partial_z v_1\right] = 0 \qquad (C\,3\,b)$$
$$(1-\Phi)\partial_z p_f = 0 \qquad (C\,3\,c)$$
$$-\partial_z\left[\Phi\eta_s\partial_z v_1\right] = 0 \qquad (C\,3\,d)$$
$$-\partial_z p_c = 0 \qquad (C\,3\,e)$$

and

$$p_c = \eta_n\left[(\partial_z v_1)^2\right]^{1/2} \qquad (C\,3\,f)$$

and no-slip conditions at $z = 0$

$$v_1 = 0, \quad w_1 = 0, \quad w_2 = 0. \qquad (C\,3\,g)$$

We see immediately that $w_2 = 0$, which provides, via matching, the boundary condition for the drift-flux model at $y = 1/2$ as claimed in the text.

Appendix D Lost of hyperbolicity

The non-viscous one-pressure two-fluid system contains an ill-posedness, that shows in the occurrence of complex characteristics in the system and a subsequent lost of hyperbolicity in time, c.f. [21]. This discussion is not obsolete for models including viscous terms as the instability reappears in the long-wave limit, c.f. [27]. Although the problem is known for decades, no universal accepted solution has been presented as of now [21].

In order to circumvent the problem of lost hyperbolicity, we can introduce a modified collision pressure p_c^* of the form

$$p_c^* = \eta_n(\phi_s)|\dot{\boldsymbol{\gamma}}_s| + \Delta p^*\phi_s, \qquad (D\,1)$$

where Δp^* is a constant regularization parameter, that should be chosen, such that

$$\Delta p^* > \boldsymbol{w}^2. \tag{D2}$$

We like to emphasize this regularization is done on purely mathematical reasons and is not based on a physical derivation. However, as the asymptotics for the stationary and time-dependent cases use a scale of the form

$$\boldsymbol{w} = \varepsilon \boldsymbol{w}^*, \tag{D3}$$

the regularization parameter will not appear for the considered orders of approximation. Thus, the proposed drift-flux model remains valid when used in connection with the regularization.

References

[1] G. K. Batchelor and J. T. Green. The determination of the bulk stress in a suspension of spherical particles to order c^2. *J. Fluid Mech.*, 56(03):401–427, 1972.

[2] François Boyer, Élisabeth Guazzelli, and Olivier Pouliquen. Unifying suspension and granular rheology. *Phys. Rev. Lett.*, 107(18):188301, October 2011.

[3] Christopher E. Brennen. *Fundamentals of Multiphase Flow*. Cambridge University Press, 2005.

[4] H. C. Brinkman. A calculation of the viscous force exerted by a flowing fluid on a dense swarm of particles. *Appl. Sci. Res.*, 1(1):27–34, 1949.

[5] C. Cassar, M. Nicolas, and O. Pouliquen. Submarine granular flows down inclined planes. *Phys. Fluids*, 17(10):103301, 2005.

[6] Andrea W. Chow, Steven W. Sinton, Joseph H. Iwamiya, and Thomas S. Stephens. Shear-induced particle migration in Couette and parallel-plate viscometers: NMR imaging and stress measurements. *Phys. Fluids*, 6(8):2561–2576, 1994.

[7] Benjamin P. Cook, Andrea L. Bertozzi, and A. E. Hosoi. Shock solutions for particle-laden thin films. *SIAM Journal on Applied Mathematics*, 68(3):760–783, Jan 2008.

[8] John de Bruyn. Unifying liquid and granular flow. *Physics*, 4:86, October 2011.

[9] Donald Allen Drew. Mathematical modeling of two-phase flow. *Annu. Rev. Fluid Mech.*, 15(1):261–291, 1983.

[10] Donald Allen Drew and Stephen L. Passman. *Theory of Multicomponent Fluids*, volume 135 of *Applied Mathematical Sciences*. Springer, 1999.

[11] Donald Allen Drew and Lee A. Segel. Averaged equations for two-phase media. *Stud. Appl. Math.*, 50(2):205–231, 1971.

[12] Albert Einstein. Eine neue Bestimmung der Moleküldimensionen. *Ann. Phys. (Berlin)*, 324(2):289–306, 1906.

[13] F. Gadalamaria and A. Acrivos. Shear-induced structure in a concentrated suspension of solid spheres. *J. Rheol.*, 24(6):799–814, 1980.

[14] R. E. Hampton. Migration of particles undergoing pressure-driven flow in a circular conduit. *J. Rheol.*, 41(3):621–640, May 1997.

[15] Kai Hiltunen, Ari Jäsberg, Sirpa Kallio, Hannu Karema, Markku Kataja, Antti Koponen, Mikko Manninen, and Veikko Taivassalo. *Multiphase Flow Dynamics*, volume 722. VTT Publications, 2009.

[16] Lucio Isa, Rut Besseling, and Wilson C. K. Poon. Shear zones and wall slip in the capillary flow of concentrated colloidal suspensions. *Phys. Rev. Lett.*, 98:198305, May 2007.

[17] Mamoru Ishii and Takashi Hibiki. *Thermo-Fluid Dynamics of Two-Phase Flow*. Springer, 2011.

[18] James T. Jenkins and David F. McTigue. Transport processes in concentrated suspensions: The role of particle fluctuations. In Daniel D. Joseph and David G. Schaeffer, editors,

Two Phase Flows and Waves, number 26 in The IMA Volumes in Mathematics and Its Applications, pages 70–79. Springer New York, January 1990.

[19] Nikolay Ivanov Kolev. *Multiphase Flow Dynamics 1: Fundamentals*. Multiphase Flow Dynamics. Springer-Verlag Berlin Heidelberg, 2005.

[20] David Leighton and Andreas Acrivos. Shear-induced migration of particles in concentrated suspensions. *J. Fluid Mech.*, 181(1):415–439, 1987.

[21] Daniel Lhuillier, Chih-Hao Chang, and Theo G. Theofanous. On the quest for a hyperbolic effective-field model of disperse flows. *J. Fluid Mech.*, 731:184–194, Aug 2013.

[22] Ryan M. Miller, John P. Singh, and Jeffrey F. Morris. Suspension flow modeling for general geometries. *Chem. Eng. Sci.*, 64(22):4597–4610, 2009.

[23] Jeffrey F. Morris and Fabienne Boulay. Curvilinear flows of noncolloidal suspensions: The role of normal stresses. *J. Rheol.*, 43:1213–1237, 1999.

[24] N. Murisic, B. Pausader, D. Peschka, and A. L. Bertozzi. Dynamics of particle settling and resuspension in viscous liquid films. *J. Fluid Mech.*, 717:203–231, Feb 2013.

[25] Prabhu R. Nott and John F. Brady. Pressure-driven flow of suspensions: simulation and theory. *J. Fluid Mech.*, 275(1):157–199, 1994.

[26] Ronald J. Phillips, Robert C. Armstrong, Robert A. Brown, Alan L. Graham, and James R. Abbott. A constitutive equation for concentrated suspensions that accounts for shear-induced particle migration. *Phys. Fluids A*, 4(1):30–40, January 1992.

[27] A. Prosperetti and A.V. Jones. The linear stability of general two-phase flow models - ii. *International Journal of Multiphase Flow*, 13(2):161–171, Mar 1987.

[28] Arun Ramachandran. A macrotransport equation for the particle distribution in the flow of a concentrated, non-colloidal suspension through a circular tube. *J. Fluid Mech.*, 734:219–252, 11 2013.

[29] Jonathan J. Stickel and Robert L. Powell. Fluid mechanics and rheology of dense suspensions. *Annu. Rev. Fluid Mech.*, 37(1):129–149, January 2005.

[30] Martin Trulsson, Bruno Andreotti, and Philippe Claudin. Transition from the viscous to inertial regime in dense suspensions. *Phys. Rev. Lett.*, 109(11):118305, 2012.

[31] Stephen Whitaker. Flow in porous media I: A theoretical derivation of Darcy's law. *Trans. Porous Media*, 1(1):3–25, 1986.

[32] Stephen Whitaker. *The Method of Volume Averaging*, volume 13. Springer, 1998.

[33] Junjie Zhou, B. Dupuy, A. Bertozzi, and A. Hosoi. Theory for shock dynamics in particle-laden thin films. *Physical Review Letters*, 94(11):117803, Mar 2005.